

# Adaptive Robotic Tool-Tip Control Learning Considering Online Changes in Grasping State

Kento Kawaharazuka<sup>1</sup>, Kei Okada<sup>1</sup>, and Masayuki Inaba<sup>1</sup>

**Abstract**—Various robotic tool manipulation methods have been developed so far. However, to our knowledge, none of them have taken into account the fact that the grasping state such as grasping position and tool angle can change at any time during the tool manipulation. In addition, there are few studies that can handle deformable tools. In this study, we develop a method for estimating the position of a tool-tip, controlling the tool-tip, and handling online adaptation to changes in the relationship between the body and the tool, using a neural network including parametric bias. We demonstrate the effectiveness of our method for online change in grasping state and for deformable tools, in experiments using two different types of robots: axis-driven robot PR2 and tendon-driven robot MusashiLarm.

## I. INTRODUCTION

Tool-use is one of the essential human abilities. So far, various studies have been conducted on the elements necessary for robotic tool-use, such as tool recognition [1], tool understanding [2], tool selection [3], tool manipulation [4], and tool generation [5]. Among these, robotic tool manipulation learning is one of the most important points in the actual robot operation. There are various stages of tool manipulation, including grasping a tool, understanding the positional relationship between the tool and the body, and planning the tool manipulation. For tool grasping, methods using kinematics and dynamics models [6], [7] and learning methods [8] are considered. For the understanding of the positional relationship between the tool and the body, most of the methods [9], [10] obtain the linear transformation or Jacobian between the hand and tool postures. For tool manipulation planning, there are several methods such as optimization-based motion planning [11], deep learning-based motion planning [12], and methods using simple tool trajectory input and whole body inverse kinematics [13]. There are also methods to solve these problems simultaneously by imitation learning [14], [15], reinforcement learning [16], and self-supervised learning [17], [18].

However, none of them have taken into account the fact that the grasping state such as grasping position and tool angle can change at any time during the tool manipulation. In addition, there are few studies that can handle deformable tools. Previous studies have basically dealt with only the state in which a rigid tool is fixed to the robot body. Therefore, in this study, we develop a method that can handle both rigid and deformable tools by learning the relationship between the

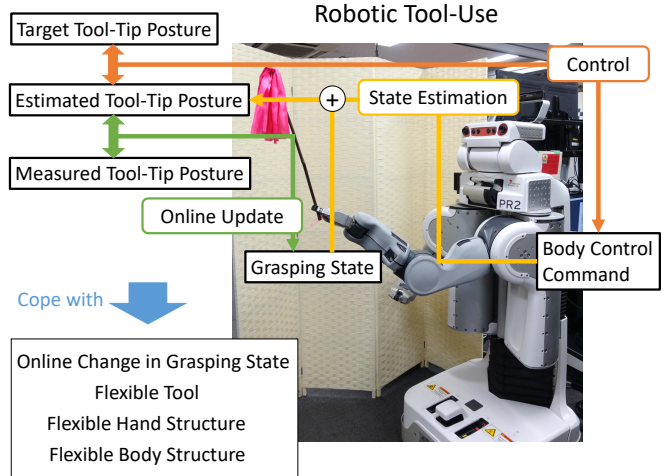


Fig. 1. The concept of this study. In robotic tool-use, a tool-tip posture is estimated from the body control command and grasping state, the body control command is calculated from the loss between the target and estimated tool-tip postures, and grasping state is updated online from the loss between the estimated and measured tool-tip postures. This study can also cope with the online change in grasping state and flexible tool, hand, and body structures.

control command of the robot body and the tool-tip position using a neural network. By using parametric bias [19], [20], the current grasping state, which cannot be obtained directly from the sensor information, is implicitly estimated online, and the control command for tool manipulation is changed based on the estimated grasping state. This system will be able to handle grasping states that can change at any time due to external forces, and deformable tools such as a long, flexible rod or a hose. We also apply our method to musculoskeletal humanoids [21], [22], which are flexible and more difficult to modelize for the grasping state.

Note that the parametric bias [19], [20] is an additional bias parameter of neural network, which can extract multiple attractor dynamics from various motion data, mostly used in imitation learning. In the context of imitation learning, there are some examples to embed implicit tool differences into parametric bias [23]. In this study, by using parametric bias instead of directly using the length and angle of the tool for a neural network, the need for annotation of the grasping state can be eliminated when creating the dataset, and deformable tools and complex grasping states can be handled. “Grasping state” in this study is defined as an implicit expression of various grasping states including grasping position, tool angle, etc., by parametric bias.

Possible alternatives to our method are (1) a method using visual or tactile feedback, and (2) a method using

<sup>1</sup> The authors are with the Department of Mechano-Informatics, Graduate School of Information Science and Technology, The University of Tokyo, 7-3-1 Hongo, Bunkyo-ku, Tokyo, 113-8656, Japan. [kawaharazuka, k-okada, inaba]@jsk.t.u-tokyo.ac.jp

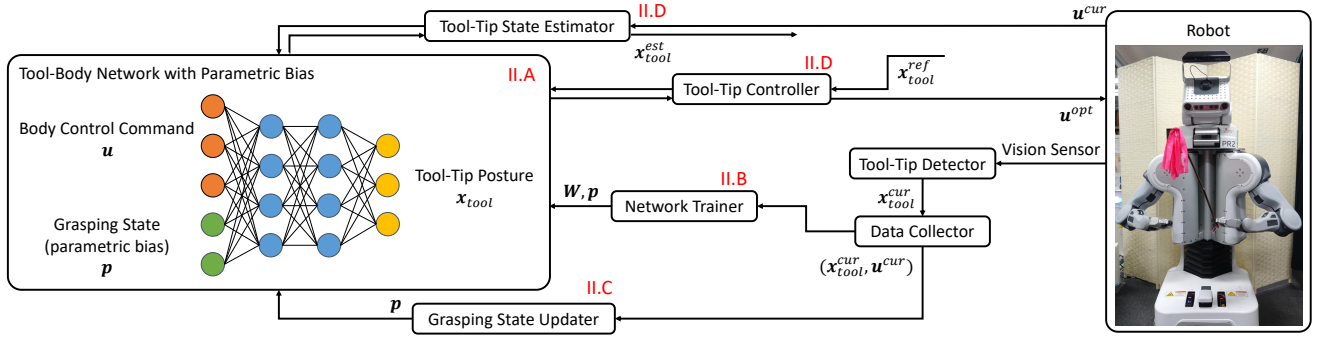


Fig. 2. The overall software system: the network structure of TBNPB, network trainer of TBNPB, online grasping state updater through parametric bias, tool-tip state estimator, and tool-tip controller.

a geometric model to estimate the grasping state. For (1), we can consider tactile feedback that can robustly respond to unexpected changes in the grasping state by storing or learning the sensor value transitions during tool-use [24], [25], and visual feedback for the tool-tip position. For (2), a simple method to determine the grasping position and tool angle from the relationship between the hand position and the tool-tip position using a geometric model of the tool can be considered. We can say that (1) is a method to compensate the grasping state by sensor feedback without estimating it, and (2) is a method to use the tool by understanding the grasping state from the geometric model. However, (1) cannot deal with deformable tools and complex robot structures where Jacobian between the control command and the target state to be controlled is not obvious. In addition, the scope of application of (1) is different from that of this study because (1) mainly follows the human demonstration and does not modelize the tool or grasping state. There is also a tool-tip control with sensor feedback using imitation learning [26], but there is no example of adaptation to changes in the grasping state of a tool. Since (2) assumes a geometric model, it cannot handle deformable tools or complex grasping states. In contrast, this study provides a general-purpose model that can be applied to complex and flexible bodies and tools by modeling the relationship between the body and tool using a neural network that can consider implicit grasping states.

This study is organized as follows. In Section II, we describe the network structure of the Tool-Body Network with Parametric Bias (TBNPB), its training, online update of grasping state, and tool-tip position estimation and control. In Section III, we confirm the effectiveness of this study on the simulation of PR2, the actual PR2, and the musculoskeletal humanoid MusashiLarm. In Section IV, we discuss the experimental results and conclude in Section V.

## II. TOOL-BODY NETWORK WITH PARAMETRIC BIAS

In this study, we call the network representing the static relationship between a tool-tip and the body control command with parametric bias, Tool-Body Network with Parametric Bias (TBNPB). The overall system of this study surrounding TBNPB is shown in Fig. 2. First, the network structure of TBNPB is constructed (Section II-A), and TBNPB is trained offline (Section II-B). Second, the grasping state is updated

online through parametric bias (Section II-C), and the tool-tip is estimated and controlled using TBNPB (Section II-D).

### A. Network Structure of TBNPB

The network structure of TBNPB is simple and can be expressed as follows,

$$\mathbf{x}_{tool} = \mathbf{h}(\mathbf{u}, \mathbf{p}) \quad (1)$$

where  $\mathbf{x}_{tool}$  is the tool-tip position,  $\mathbf{h}$  is TBNPB,  $\mathbf{u}$  is the body control command, and  $\mathbf{p}$  is the parametric bias, which corresponds to the implicit grasping state. Although  $\mathbf{x}_{tool}$  can represent position and orientation, in this study, it represents only the three-dimensional position. In this study,  $\mathbf{u}$  represents the control command of the joint angle  $\theta^{ref}$ . Parametric bias  $\mathbf{p}$  has been originally used to extract multiple attractor dynamics in time series information [20]. Therefore, it is mostly used together with recurrent neural networks, but in this study, we use this parametric bias for the static correspondence network.

In this study, the number of layers of TBNPB is 7. The number of units is set to the combined number of dimensions of  $\mathbf{u}$  and  $\mathbf{p}$  (which varies depending on the robot) for the input, 300 for all the middle 5 layers, and 3 (the number of dimension of  $\mathbf{x}_{tool}$ ) for the output. The activation function is hyperbolic tangent, and the update rule is Adam [27]. The input and output values of the network are normalized using the data obtained during training.

### B. Training of TBNPB

This section describes Data Collector and Network Trainer in Fig. 2. First, for various grasping states  $k$  ( $1 \leq k \leq K$ ;  $K$  is the total number of grasping states used for training), where the grasped angle and position of the tool are different, the data at various body control commands  $D_k = \{(\mathbf{u}, \mathbf{x}_{tool})_1, \dots, (\mathbf{u}, \mathbf{x}_{tool})_{N_k}\}$  ( $N_k$  is the number of data for grasping state  $k$ ) is collected. Also, we prepare parametric bias  $\mathbf{p}_k$  for each grasping state  $k$  (all  $\mathbf{p}_k$  are initialized to 0). Thus, the data  $D_{train} = \{(D_1, \mathbf{p}_1), \dots, (D_{N_k}, \mathbf{p}_{N_k})\}$  is collected and it is used to train  $\mathbf{h}$ . Here,  $\mathbf{p}_k$  is common for the data  $D_k$  and different variables are used for different grasping states. During the training process, the network weights  $W$  and  $\mathbf{p}_k$  are updated at the same time by the backpropagation method. In this way, the grasping state information is embedded in  $\mathbf{p}_k$ . No annotation for  $\mathbf{p}_k$  is necessary.

In this study, training procedure is performed in two stages. First, we collect data by changing the grasping state in the simulation, and calculate  $W$  and  $\mathbf{p}_k$ . Then, we initialize  $\mathbf{p}_k$  to 0, leaving only the  $W$  calculated in the simulation. Finally, we collect the data in the actual robot and perform the training again. Since the data obtained from the actual robot is small, we conduct fine-tuning.

### C. Online Update of Grasping State

This section describes Grasping State Updater in Fig. 2. Assuming that the grasping state can change at any time, we update the parametric bias  $\mathbf{p}$  online. Data is collected when the tool-tip position  $\mathbf{x}_{tool}$  is recognized and the control command  $\mathbf{u}$  differs to a certain extent from the control command  $\mathbf{u}^{prev}$  collected just before; that is, if  $\|\mathbf{u} - \mathbf{u}^{prev}\|_2 > C_{collect}$  ( $\|\cdot\|_2$  is the L2 norm and  $C_{collect}$  is the threshold). We start online update when the number of obtained data  $N_{online}$  exceeds  $N_{thre}^{online}$ , and then we update  $\mathbf{p}$  each time new data is collected. The weight  $W$  is fixed; only  $\mathbf{p}$  is updated as  $N_{batch}^{online}$  batches and  $N_{epoch}^{online}$  epochs. Here, the update rule is momentum SGD [28] with the learning rate set to 0.1. The maximum number of the data is set to  $N_{max}^{online}$  ( $N_{thre}^{online} \leq N_{max}^{online}$ ), and the data exceeding it are deleted from the oldest one. By fixing the weight  $W$  of the network and updating only the parametric bias, which has a small dimension, we can update only the grasping state while preventing overfitting.

In this study, we set  $C_{collect} = 10.0$  [deg],  $N_{thre}^{online} = 10$ ,  $N_{batch}^{online} = N_{online}$ ,  $N_{epoch}^{online} = 3$ , and  $N_{max}^{online} = 20$ . Also, the sampling rate of data collection is 5 Hz.  $C_{collect}$  should be set appropriately according to the scale of the whole motion. The larger  $N_{thre}^{online}$  is, the more stable the online update is in the early stage, but the slower the update starts, so it should be set appropriately according to the application. The larger  $N_{max}^{online}$  is, the more accurately the grasping state can be updated using a large number of data, but the slower it is to adapt to changes in the grasping state, so it should be set appropriately taking into account the tradeoff.

### D. State Estimation and Control of Tool-Tip Using TBNPB

This section describes Tool-Tip State Estimator / Controller in Fig. 2. The tool-tip state estimation is very simple and it can be calculated by merely inputting the current  $\mathbf{p}$  and the control command  $\mathbf{u}$  into  $\mathbf{h}$ . The tool-tip control is performed by optimization using the backpropagation method and gradient descent. First, we obtain the current control command  $\mathbf{u}^{cur}$  and use it as the initial value of the control command  $\mathbf{u}^{opt}$  to be optimized. Next, we perform the optimization as follows,

$$\mathbf{x}_{tool}^{est} = \mathbf{h}(\mathbf{u}^{opt}, \mathbf{p}) \quad (2)$$

$$L = \|\mathbf{x}_{tool}^{est} - \mathbf{x}_{tool}^{ref}\|_2 + \alpha L_{const}(\mathbf{u}^{opt}) \quad (3)$$

$$\mathbf{u}^{opt} \leftarrow \mathbf{u}^{opt} + \gamma \partial L / \partial \mathbf{u}^{opt} \quad (4)$$

where  $\mathbf{x}_{tool}^{ref}$  is the target tool-tip position,  $L_{const}$  is the constraint on the control command  $\mathbf{u}$ ,  $\alpha$  is the weight of the loss function, and  $\gamma$  is the learning rate. For  $L_{const}$ , for

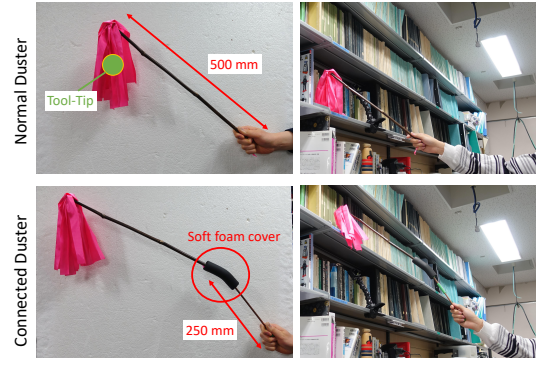


Fig. 3. The tools used in this study: normal and connected dusters.

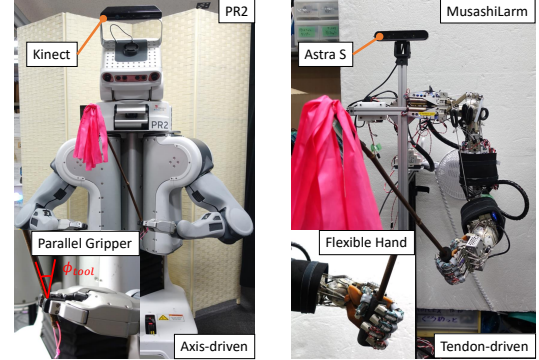


Fig. 4. The robots used in this study: PR2 with the parallel gripper and the musculoskeletal arm MusashiLarm with the flexible hand.

example, if we want  $\mathbf{u}$  to be as close as possible to the current control command, we can set it to  $\|\mathbf{u}^{opt} - \mathbf{u}^{cur}\|_2$ , or if we do not want to move a certain joint, we can constrain it by giving a loss function only for that joint. For  $\gamma$ , in this study, we try  $N_{batch}^{control}$  number of  $\gamma$  from 0 to  $\gamma^{max}$  by line search and adopt the one with the smallest loss, repeating  $N_{epoch}^{control}$  times ( $\gamma^{max}$  is the maximum value of  $\gamma$ ). Using the finally obtained  $\mathbf{u}^{opt}$ , the tool-tip position can be controlled.

In this study, we set  $\gamma^{max} = 0.5$ ,  $N_{batch}^{control} = 30$ , and  $N_{epoch}^{control} = 10$ .

## III. EXPERIMENTS

### A. Experimental Setup

In this study, we conduct experiments using a duster, which removes dust from shelves and objects by controlling the tool-tip position (Fig. 3). A colored cloth is attached to the tool-tip, and the tool-tip position is recognized by extracting the color of the cloth. The cloth of the duster drops from the tip of the stick in the direction of gravity, and the tool-tip position cannot be linearly transformed from the hand posture. As a more difficult condition, we also use another duster of which the length is increased by attaching an additional stick to it in the PR2 experiment. We call this a “connected duster”. The normal duster and the additional stick are connected by a flexible foam cover, so that the tool-tip position changes greatly depending on the angle at which the duster is held. The stick length of the normal duster is 500 mm, that of the colored cloth is 200 mm, and that of the additional stick is 250 mm.

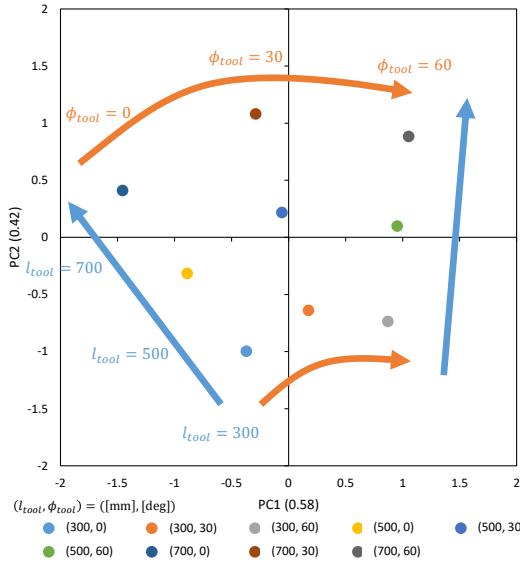


Fig. 5. Parametric bias trained in PR2 simulation experiment.

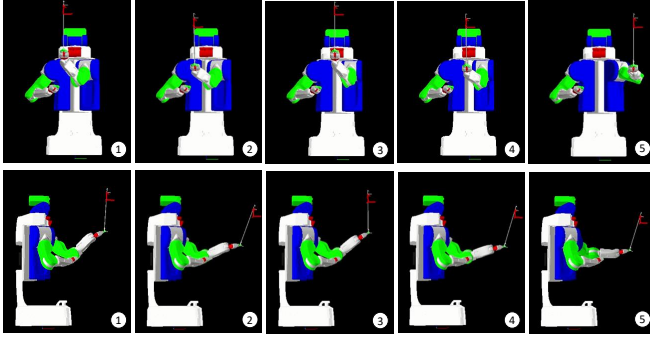


Fig. 6. Duster-use motion for PR2 experiments.

In the experiments of this study, we use the simulation and the actual robot of the wheeled axis-driven humanoid PR2 and the actual robot of the musculoskeletal arm MusashiLarm [22] (Fig. 4). In the PR2 / MusashiLarm, the head is equipped with a Kinect (Microsoft, Corp.) / Astra S (Orbbec 3D Technology International, Inc.) depth camera. Point clouds of the tool-tip are extracted through color filtering, euclidean clustering is performed, and the center of the largest cluster is set as the tool-tip position. The hand of PR2 is a parallel gripper, and the grasping angle  $\phi_{tool}$  shown in Fig. 4 and the grasping position of the tool are mainly changed during the tool-use. On the other hand, the hand of MusashiLarm is a flexible hand using machined springs, and it is difficult to parameterize the grasping state.

### B. PR2 Simulation Experiment

We conduct an experiment using the geometric simulator of PR2. First, we attach a long thin object to the hand to represent the duster, and obtain data by changing the grasping position (expressed as the length of tool stick from the hand)  $l_{tool}$  and the grasping angle (expressed as the angle perpendicular to the parallel gripper with one degree of freedom)  $\phi_{tool}$ . Since the cloth of the duster hangs down from the tip of the stick in the direction of gravity, we simulate the tool-tip at -100 mm in the  $z$ -direction from the tip of

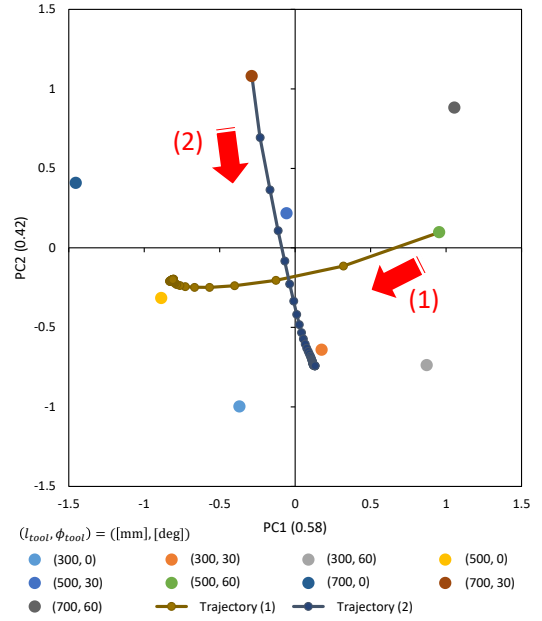


Fig. 7. Transition of parametric bias when changing grasping state: (1)  $(l_{tool}, \phi_{tool}) = (500, 60) \rightarrow (500, 0)$ , (2)  $(l_{tool}, \phi_{tool}) = (700, 30) \rightarrow (300, 30)$  in PR2 simulation experiment with grasping state updater.

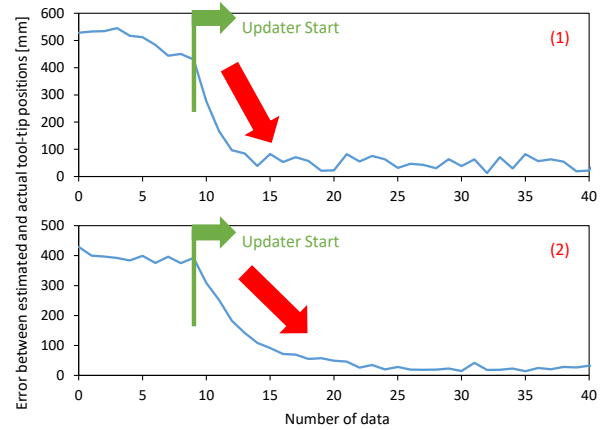


Fig. 8. Transition of state estimation error of tool-tip position when changing grasping state: (1)  $(l_{tool}, \phi_{tool}) = (500, 60) \rightarrow (500, 0)$ , (2)  $(l_{tool}, \phi_{tool}) = (700, 30) \rightarrow (300, 30)$  in PR2 simulation experiment with grasping state updater.

the stick. We change grasping state as  $l_{tool} = \{300, 500, 700\}$  [mm] and  $\phi_{tool} = \{0, 30, 60\}$  [deg]. Next, the joint angle limit is determined, and within the range, the joint angles are randomly sampled for each grasping state, and the data  $D_{train}$  is obtained. The total number of  $D_{train}$  is 9000, and TBNPB is trained as 300 batches and 300 epochs. Note that  $\mathbf{u}$  is seven-dimensional and  $\mathbf{p}$  is two-dimensional. The parametric bias  $p_k$  obtained here is represented in two-dimensional space through principal component analysis (PCA) as shown in Fig. 5. We can see that the parametric bias is aligned neatly along the magnitude of  $l_{tool}$  and  $\phi_{tool}$ . The larger  $l_{tool}$  is, the larger the difference in parametric bias due to the change in  $\phi_{tool}$  is, which is consistent with the fact that a longer tool has a larger change in tool-tip position depending on the angle.

Next, we experiment on the behavior of grasping state updater and tool-tip state estimator. We conduct experiments

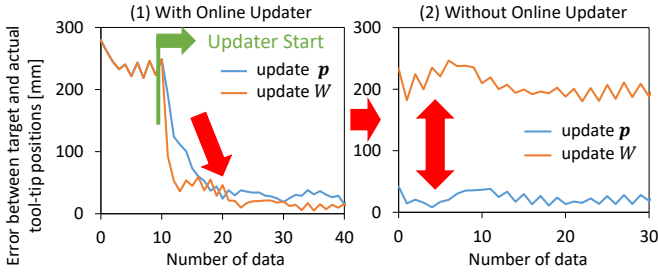


Fig. 9. Transition of control error of tool-tip position when changing grasping state:  $(l_{tool}, \phi_{tool}) = (500, 30) \rightarrow (500, 60)$  in PR2 simulation experiment with online updaters of updating  $\mathbf{p}$  or  $W$ . The right experiment is conducted at different posture from the trained one without online updaters.

for two cases: (1) when the grasping state is changed from  $(l_{tool}, \phi_{tool}) = (500, 60)$  to  $(l_{tool}, \phi_{tool}) = (500, 0)$ , and (2) when the grasping state is changed from  $(l_{tool}, \phi_{tool}) = (700, 30)$  to  $(l_{tool}, \phi_{tool}) = (300, 30)$ . The motion of shaking the duster is shown in Fig. 6 (for the case of  $(l_{tool}, \phi_{tool}) = (500, 30)$ ). This is a motion in which we determine a reference point of the tool-tip (with the center of wheeled cart of PR2 as the origin, e.g.  $(800, -100, 1600)$  [mm] for  $(l_{tool}, \phi_{tool}) = (500, 30)$ ), and alternately move the tool-tip by 100 mm in the  $y$  direction, then move and return  $(200, -200)$  [mm] in the  $(x, z)$  direction, while solving inverse kinematics. If the movement in the  $y$  direction exceeds 500 mm, move in the opposite direction. The transition of parametric bias during this motion is shown in Fig. 7, and the transition of the state estimation error of the tool-tip position is shown in Fig. 8. It can be seen that for both (1) and (2), the parametric bias is gradually approaching the area around the current grasping state obtained at training. In addition, the state estimation error of the tool-tip position also decreases gradually. When more than 20 data points were collected, the average estimation errors were 52.2 mm for (1) and 25.9 mm for (2).

Finally, we experiment on the tool-tip controller. Starting from the state where parametric bias is  $(l_{tool}, \phi_{tool}) = (500, 30)$  obtained at training, and setting  $(l_{tool}, \phi_{tool}) = (500, 60)$ , we compare the control error of the tool-tip position when using the grasping state updater (update  $\mathbf{p}$ ) or when  $\mathbf{p}$  is fixed and  $W$  is updated (update  $W$ ). The former corresponds to updating only  $\mathbf{p}$ , while the latter corresponds to updating the weight  $W$  without  $\mathbf{p}$ , as in ordinary online learning (note that the learning rate is set to 0.01 for the latter). The behavior is the same as that of Fig. 6. Here, the joint angle  $\mathbf{u}^{orig}$  of Fig. 6 generated as  $(l_{tool}, \phi_{tool}) = (500, 30)$  is used as a reference, so that we set  $\alpha = 0.3$  and  $L_{const} = \|\mathbf{u}^{opt} - \mathbf{u}^{orig}\|_2$ . The transition of the control error of the tool-tip position is shown in the left figure of Fig. 9. It can be seen that the initial control error without online updaters is about 240 mm, while the control error is greatly reduced by online updaters. For more than 20 data points, the average control error is 31.5 mm for the former (update  $\mathbf{p}$ ) and 19.2 mm for the latter (update  $W$ ), and the latter, which updates the entire network, is more accurate. The transition of the control error when the online updater was stopped and the same tool-tip position trajectory was performed with completely

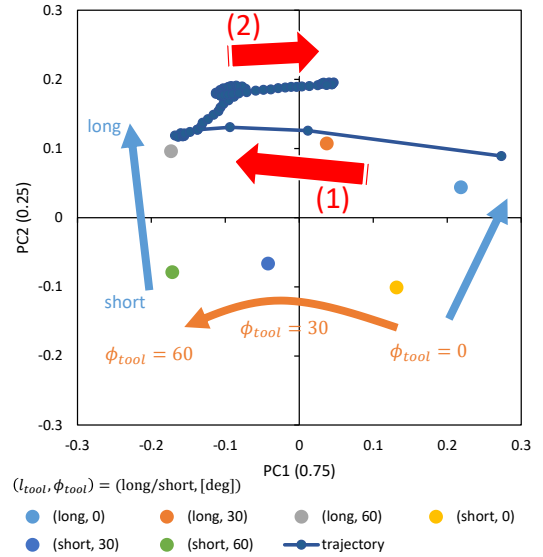


Fig. 10. Parametric bias trained in PR2 experiment with the normal duster and its trajectory in the tool-tip control experiment with grasping state updater.

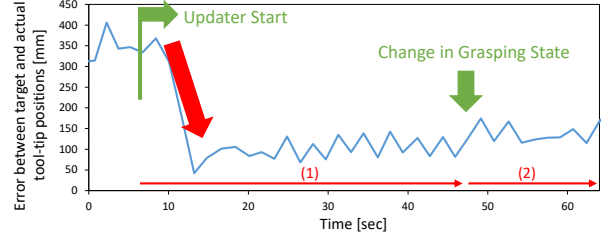


Fig. 11. Transition of control error of tool-tip position in tool-tip control experiment of PR2 with the normal duster.

different  $\mathbf{u}^{orig}$  due to different tool-tip rotational constraints is shown in the right figure of Fig. 9. After updating only  $\mathbf{p}$ , the control error is 22.6 mm on average, while it is 207 mm after updating  $W$ . In the case of updating only  $\mathbf{p}$ , the grasping state updater is effective in other joint angles, while in the case of updating  $W$ , the control error is larger in other joint angles due to over-fitting to the data used for online learning.

### C. PR2 Experiment

We perform experiments using the actual robot PR2. We perform the motion of Fig. 6 performed in Section III-B three times while changing the reference point of the tool-tip to obtain the data. The above procedure is repeated while changing the grasping state, and TBNPB is trained using about 1500 data points obtained, with 30 batches and 100 epochs. We fine-tuned the model obtained in Section III-B as described in Section II-B. Since the grasping state is trained implicitly, we roughly create the states of holding the tool long or short and  $\phi_{tool} = \{0, 30, 60\}$ , and collect the data. The distribution of parametric bias obtained by fine-tuning is shown in Fig. 10. In a similar but different form from Fig. 5, we can see that the parametric bias is neatly distributed along long or short  $l_{tool}$  and  $\phi_{tool} = \{0, 30, 60\}$ . The results of the experiment on tool-tip control conducted in the same way as Fig. 9 are shown in Fig. 11. Initially, the control error

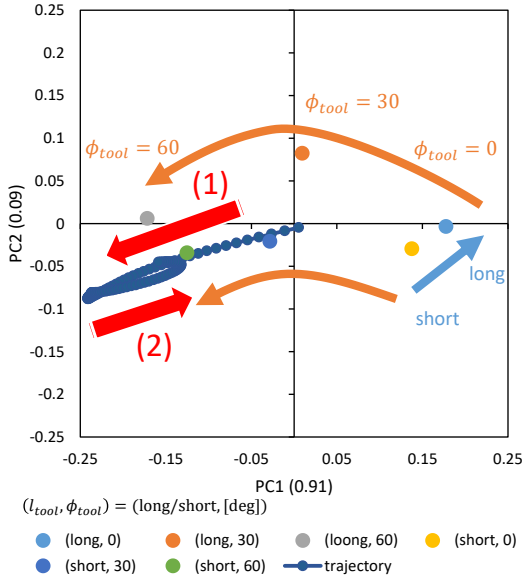


Fig. 12. Parametric bias trained in PR2 experiment with the connected duster and its trajectory in the tool-tip control experiment with grasping state updater.

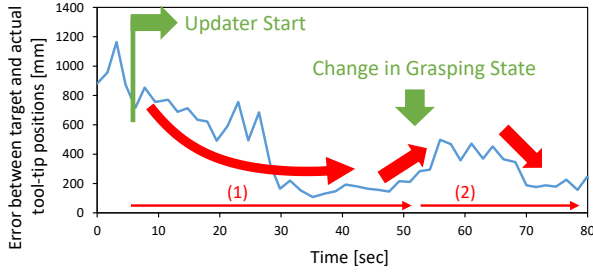


Fig. 13. Transition of control error of tool-tip position in tool-tip control experiment of PR2 with the connected duster.

is large, about 350 mm, because the grasping state is not known, but after the number of data exceeds  $N_{thre}^{nonline}$  and the grasping state updater is executed, the control error suddenly decreases and drops to about 100 mm. After that, the control error did not change significantly even though we changed the grasping state by manually applying external force to the tool. The transition of parametric bias here is shown in “trajectory” of Fig. 10, where (1) is the transition after the start of the updater and (2) is the transition after the change of the grasping state. We can see that parametric bias is automatically and correctly updated by detecting the change in the grasping state.

Next, we perform an experiment using PR2 with the connected duster. As in the previous experiment, we collect data and train TBNPB, and the parametric bias obtained is shown in Fig. 12. The parametric bias is considered to have a form that varies more with  $\phi_{tool}$  than with short / long  $l_{tool}$ , compared to Fig. 10, because it bends greatly as the angle of the tool increases. The results of the same tool-tip control experiment as before are shown in Fig. 13. The initial control error is about 890 mm, which is very large, but the grasping state gradually becomes known, and the error is reduced to about 160 mm. After that, the control error increases to about 450 mm when we change the grasping state by applying



Fig. 14. Duster-use experiment of PR2.

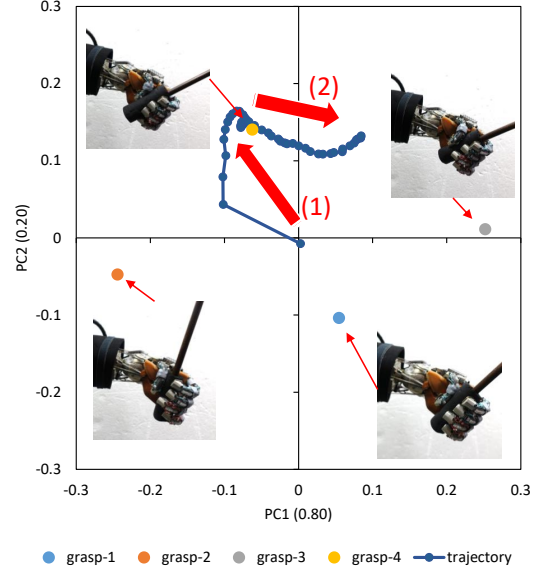


Fig. 15. Parametric bias trained in MusashiLarm experiment and its trajectory in the tool-tip control experiment with grasping state updater.

external force to the tool, but it decreases again to about 190 mm by the grasping state updater. The transition of the parametric bias here is shown in “trajectory” of Fig. 12, where (1) is the transition after the start of the updater and (2) is the transition after the change of the grasping state. For the flexible tool, we can see that the parametric bias is automatically and correctly updated by detecting the change in grasping state.

Finally, the duster-use motion of PR2 with normal duster is shown in Fig. 14. The duster-use motion is performed with a tool-tip position command such that the duster touches the objects on the shelves. At first, the duster does not touch the objects because the estimated grasping state is not correct, but after updating it, the duster correctly touches the objects and removes the dust.

#### D. MusashiLarm Experiment

We perform experiments using the actual robot MusashiLarm. In this section, as in PR2, we first collect data using the geometric simulator of MusashiLarm and train TBNPB. Here, we fixed  $l_{tool} = 500$  [mm] and defined the angle  $\psi_{tool}$  of the tool in the direction perpendicular to  $\phi_{tool}$ , and collected data with  $\phi_{tool} = \{0, 30, 60\}$  [deg] and  $\psi_{tool} = \{-30, 0, 30\}$  [deg]. Note that  $\mathbf{u}$  is 5-dimensional (2-dimensional wrist is not included) and  $\mathbf{p}$  is 2-dimensional. After that, the data is collected by the actual robot as in Section III-C (in this case, joint angle commands are converted to muscle length by [29]), and the parametric bias after fine-tuning of TBNPB is shown in Fig. 15. Unlike

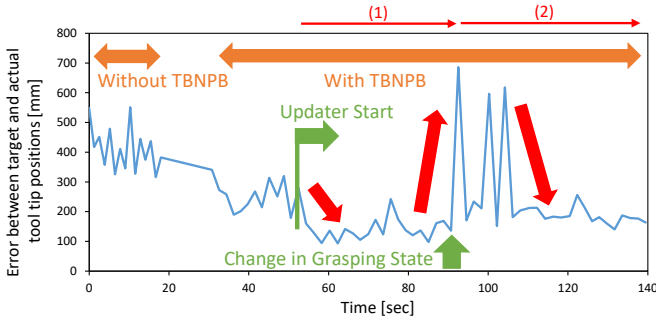


Fig. 16. Transition of control error of tool-tip position in the tool-tip control experiment of MusashiLarm.

PR2, the grasping states are complex, so the human-created grasping states used for training are denoted as grasp-{1, 2, 3, 4}. The results of the tool-tip control experiment using the TBNPB as in PR2 are shown in Fig. 16. Using the geometric model with  $\phi_{tool} = 30$  and  $\psi = 0$  without TBNPB, the control error is about 410 mm, while using TBNPB, the control error is reduced to about 260 mm. In addition, by using grasping state updater, the control error is reduced to about 120 mm. After that, the grasping state is changed by applying an external force to the tool, and the control error is greatly increased, but it is reduced to about 180 mm again by the grasping state updater.

#### IV. DISCUSSION

We discuss the results obtained from the experiments. From the simulator experiment of PR2, it is found that parametric bias self-organizes neatly according to the grasping state. They are self-organized in a way that is consistent with the fact that the longer the tool is, the larger the change of the tool-tip position due to the difference of the grasping angle is. We also found that the grasping state updater makes the current parametric bias transition to the correct value of the current grasping state. This allows the state estimation and the tool-tip position control to become more accurate than in the case without the grasping state updater. In addition, when the entire network is updated as in ordinary online learning, instead of updating only  $\mathbf{p}$  as in this study, the tool-tip position can be controlled more accurately around the learned data, but over-fitting occurs and the control error becomes larger for the untrained data. Since our grasping state updater updates only the grasping state, not the entire network, it is possible to reduce the control error for untrained data. The same tendency is observed in the actual robot of PR2, and it is possible to update the grasping state by the online updater and to reduce the control error with it. Similar results are obtained in the experiment using the connected duster, which is a flexible tool, and it is found that the method can be applied not only to rigid tools but also to deformable tools. Finally, in the experiment using MusashiLarm, we dealt with a system in which the grasping state is more ambiguous and the body is flexible. It is found that the control error is very large without TBNPB, but it is reduced by using TBNPB, and it is further reduced by updating the ambiguous grasping state. In other words,

TBNPB can be applied to flexible hands where the grasping state cannot be defined and to flexible robots where the joint angle cannot be realized precisely. In addition, depending on how the data are collected, irreproducible initialization and deterioration over time, which are specific to flexible bodies, can be included in the parametric bias as in [30]. Therefore, it is found that the estimation and control of the tool-tip, and update of the grasping state are possible for rigid axis-driven robots, flexible tendon-driven robots, various robotic hands, rigid tools, and deformable tools.

The main limitations of this study are (1) data collection, (2) range of tool types, and (3) control error. Regarding (1), since we have to obtain data for each tool, the current method does not scale up to many tools. On the other hand, it should be possible to embed the tool types into the parametric bias as well as the grasping state. In this case, we need to obtain a large amount of data (i.e., various tool types and various grasping states), but we can infer new tools and grasping states that correspond to the internally dividing points of the training data. In addition, we think that obtaining a large amount of prior tool data by using simulation is one direction. Regarding (2), this study can currently handle rigid and elastic tools, but it is difficult to use tools with melting or breaking properties. In this study, the mapping from  $\mathbf{u}$  to  $\mathbf{x}_{tool}$  is embedded in the weights  $\mathbf{W}$ , and the rest is embedded in  $\mathbf{p}$ . Therefore, tools such as rigid and elastic bodies, for which  $\mathbf{x}_{tool}$  can be calculated from  $\mathbf{u}$  using the effect of gravity or the structure of the tool, can be treated in the same way as in this study. On the other hand, for tools with melting or breaking properties, where  $\mathbf{x}_{tool}$  is not uniquely determined from  $\mathbf{u}$  due to transformations, those transformations will be embedded in  $\mathbf{p}$ . In this case, the changes in the tool structure and the grasping state will be embedded in the same  $\mathbf{p}$ , which is likely to make this study less useful. Regarding (3), since the tool-tip shape of the duster is amorphous and the observation error is large, the error of the experimental results is relatively large. Although this was not a problem because the duster does not require such precise operation, the control error becomes a big problem when handling tools such as drills and saws. The inference accuracy of our network mainly depends on the recognition accuracy of the tool-tip and the motion range of the tool-tip in the whole operation. Since the smaller the whole motion is, the relatively higher the inference accuracy for the tool-tip position will be, we think that drills and hammers can be handled by making the whole motion small. Since our method learns the relationship between the body and the tool itself, once the grasping state is correctly updated, the robot can look away from the tool, which is the difference from visual feedback, in which the robot must continue to look at the tool. However, if we want to perform more precise motions, we should consider using TBNPB for tool-tip control to some extent, and then using it together with visual feedback.

The application of this research is not limited to the tool-tip control. For a group of sensors and actuators that have some static relationships, it is possible to learn and use

these relationships while embedding implicit and difficult-to-observe information into parametric bias by using this study. This is the first method that brings parametric bias, which has been used in imitation learning, to static relationships. Moreover, since it uses a neural network, it is very easy to integrate not only the relationship between two sensors but also other sensors. In the future, we would like to learn the relationship between various sensors, including contact sensors and torque sensors. We would also like to try new tasks such as controlling the water coming out of a hose.

## V. CONCLUSION

In this study, we constructed a network to estimate the tool-tip position from the body control command, and developed a method to control the tool-tip position using back-propagation. By including parametric bias, implicit variables related to the grasping state are embedded in the network, and the network can adapt to the online changes in the grasping state through online learning. In addition, by using a neural network instead of a linear transformation, we have confirmed that the system can handle deformable tools and bodies with different structures such as axis-driven and tendon-driven robots. In the future, we would like to discuss the extension to the dynamic tool-use and the integration with redundant sensors such as contact and torque sensors.

## REFERENCES

- [1] E. Huber and K. Baker, "Using a hybrid of silhouette and range templates for real-time pose estimation," in *Proceedings of the 2004 IEEE International Conference on Robotics and Automation*, 2004, pp. 1652–1657.
- [2] Y. Zhu, Y. Zhao, and S. Zhu, "Understanding tools: Task-oriented object modeling, learning and recognition," in *Proceedings of the 2015 IEEE International Conference on Computer Vision and Pattern Recognition*, 2015, pp. 2855–2864.
- [3] K. P. Tee, J. Li, L. T. P. Chen, K. W. Wan, and G. Ganesh, "Towards Emergence of Tool Use in Robots: Automatic Tool Recognition and Use Without Prior Tool Learning," in *Proceedings of the 2018 IEEE International Conference on Robotics and Automation*, 2018, pp. 6439–6446.
- [4] M. Toussaint, K. Allen, K. Smith, and J. Tenenbaum, "Differentiable Physics and Stable Modes for Tool-Use and Manipulation Planning," in *Proceedings of the 2018 Robotics: Science and Systems*, 2018.
- [5] K. Kawaharazuka, T. Ogawa, and C. Nabeshima, "Tool Shape Optimization through Backpropagation of Neural Network (in press)," in *Proceedings of the 2020 IEEE/RSJ International Conference on Intelligent Robots and Systems*, 2020.
- [6] A. T. Miller and P. K. Allen, "Graspit! A versatile simulator for robotic grasping," *IEEE Robotics Automation Magazine*, vol. 11, no. 4, pp. 110–122, 2004.
- [7] Y. Xue and Y. B. Jia, "Gripping a Kitchen Knife on the Cutting Board," in *Proceedings of the 2020 IEEE/RSJ International Conference on Intelligent Robots and Systems*, 2020, pp. 9226–9231.
- [8] J. Mahler, M. Matl, V. Satish, M. Danielczuk, B. DeRose, S. McKinley, and K. Goldberg, "Learning ambidextrous robot grasping policies," *Science Robotics*, vol. 4, no. 26, 2019.
- [9] H. Hoffmann, Z. Chen, D. Earl, D. Mitchell, B. Salemi, and J. Sinapov, "Adaptive robotic tool use under variable grasps," *Robotics and Autonomous Systems*, vol. 62, no. 6, pp. 833–846, 2014.
- [10] C. Nabeshima, Y. Kuniyoshi, and M. Lungarella, "Adaptive body schema for robotic tool-use," *Advanced Robotics*, vol. 20, no. 10, pp. 1105–1126, 2006.
- [11] K. Fang, Y. Zhu, A. Garg, A. Kurenkov, V. Mehta, L. Fei-Fei, and S. Savarese, "Learning Task-Oriented Grasping for Tool Manipulation with Simulated Self-Supervision," in *Proceedings of the 2018 Robotics: Science and Systems*, 2018.
- [12] A. Xie, F. Ebert, S. Levine, and C. Finn, "Improvisation through Physical Understanding: Using Novel Objects as Tools with Visual Foresight," arXiv preprint arXiv:1904.05538, 2019.
- [13] K. Okada, M. Kojima, Y. Sagawa, T. Ichino, K. Sato, and M. Inaba, "Vision based behavior verification system of humanoid robot for daily environment tasks," in *Proceedings of the 2006 IEEE-RAS International Conference on Humanoid Robots*, 2006, pp. 7–12.
- [14] K. Takahashi, K. Kim, T. Ogata, and S. Sugano, "Tool-body assimilation model considering grasping motion through deep learning," *Robotics and Autonomous Systems*, vol. 91, pp. 115–127, 2017.
- [15] N. Saito, T. Ogata, S. Funabashi, H. Mori, and S. Sugano, "How to Select and Use Tools? : Active Perception of Target Objects Using Multimodal Deep Learning," *IEEE Robotics and Automation Letters*, vol. 6, no. 2, pp. 2517–2524, 2021.
- [16] M. Eppe, P. D. H. Nguyen, and S. Wermter, "From Semantics to Execution: Integrating Action Planning With Reinforcement Learning for Robotic Causal Problem-Solving," *Frontiers in Robotics and AI*, vol. 6, p. 123, 2019.
- [17] K. Fang, Y. Zhu, A. Garg, A. Kurenkov, V. Mehta, L. Fei-Fei, and S. Savarese, "Learning task-oriented grasping for tool manipulation from simulated self-supervision," *The International Journal of Robotics Research*, vol. 39, no. 2-3, pp. 202–216, 2020.
- [18] T. Mar, V. Tikhonoff, and L. Natale, "What Can I Do With This Tool? Self-Supervised Learning of Tool Affordances From Their 3-D Geometry," *IEEE Transactions on Cognitive and Developmental Systems*, vol. 10, no. 3, pp. 595–610, 2018.
- [19] J. Tani, "Self-organization of behavioral primitives as multiple attractor dynamics: a robot experiment," in *Proceedings of the 2002 International Joint Conference on Neural Networks*, 2002, pp. 489–494.
- [20] J. Tani, M. Ito, and Y. Sugita, "Self-organization of distributedly represented multiple behavior schemata in a mirror system: reviews of robot experiments using RNNPB," *Neural Networks*, vol. 17, no. 8, pp. 1273–1289, 2004.
- [21] S. Wittmeier, C. Alessandro, N. Bascarevic, K. Dalamagkidis, D. Devereux, A. Diamond, M. Jäntschi, K. Jovanovic, R. Knight, H. G. Marques, P. Milosavljevic, B. Mitra, B. Svetozarevic, V. Potkonjak, R. Pfeifer, A. Knoll, and O. Holland, "Toward Anthropomorphic Robotics: Development, Simulation, and Control of a Musculoskeletal Torso," *Artificial Life*, vol. 19, no. 1, pp. 171–193, 2013.
- [22] K. Kawaharazuka, S. Makino, K. Tsuzuki, M. Onitsuka, Y. Nagamatsu, K. Shinjo, T. Makabe, Y. Asano, K. Okada, K. Kawasaki, and M. Inaba, "Component Modularized Design of Musculoskeletal Humanoid Platform Musashi to Investigate Learning Control Systems," in *Proceedings of the 2019 IEEE/RSJ International Conference on Intelligent Robots and Systems*, 2019, pp. 7294–7301.
- [23] S. Nishide, J. Tani, T. Takahashi, H. G. Okuno, and T. Ogata, "ToolBody Assimilation of Humanoid Robot Using a Neurodynamical System," *IEEE Transactions on Autonomous Mental Development*, vol. 4, no. 2, pp. 139–149, 2012.
- [24] P. Pastor, M. Kalakrishnan, L. Righetti, and S. Schaal, "Towards Associative Skill Memories," in *Proceedings of the 2012 IEEE-RAS International Conference on Humanoid Robots*, 2012, pp. 309–315.
- [25] H. Girgin and E. Ugur, "Associative Skill Memory Models," in *Proceedings of the 2018 IEEE/RSJ International Conference on Intelligent Robots and Systems*, 2018, pp. 6043–6048.
- [26] A. Sasagawa, S. Sakaino, and T. Tsuji, "Motion Generation Using Bilateral Control-Based Imitation Learning With Autoregressive Learning," *IEEE Access*, vol. 9, pp. 20 508–20 520, 2021.
- [27] D. P. Kingma and J. Ba, "Adam: A Method for Stochastic Optimization," in *Proceedings of the 3rd International Conference on Learning Representations*, 2015, pp. 1–15.
- [28] N. Qian, "On the momentum term in gradient descent learning algorithms," *Neural Networks*, vol. 12, no. 1, pp. 145–151, 1999.
- [29] K. Kawaharazuka, K. Tsuzuki, S. Makino, M. Onitsuka, Y. Asano, K. Okada, K. Kawasaki, and M. Inaba, "Long-time Self-body Image Acquisition and its Application to the Control of Musculoskeletal Structures," *IEEE Robotics and Automation Letters*, vol. 4, no. 3, pp. 2965–2972, 2019.
- [30] K. Kawaharazuka, K. Tsuzuki, M. Onitsuka, Y. Asano, K. Okada, K. Kawasaki, and M. Inaba, "Object Recognition, Dynamic Contact Simulation, Detection, and Control of the Flexible Musculoskeletal Hand Using a Recurrent Neural Network With Parametric Bias," *IEEE Robotics and Automation Letters*, vol. 5, no. 3, pp. 4580–4587, 2020.